Skeletal Muscle of Stroke-Prone Spontaneously Hypertensive Rats Exhibits Reduced Insulin-Stimulated Glucose Transport and Elevated Levels of Caveolin and Flotillin

Declan J. James,[1,2] Fiona Cairns,[1] Ian P. Salt,[1,2] Gregory J. Murphy,[3] Anna F. Dominiczak,[2] John M.C. Connell,[2] and Gwyn W. Gould[1]

Insulin resistance is of major pathogenic importance in several common human disorders, but the underlying mechanisms are unknown. The stroke-prone spontaneously hypertensive (SHRSP) rat is a model of human insulin resistance and is characterized by reduced insulin-mediated glucose disposal and defective fatty acid metabolism in isolated adipocytes (Collison et al. [*Diabetes* 49:2222–2226, 2000]). In this study, we have examined skeletal muscle and cultured skeletal muscle myoblasts for defects in insulin action in the male SHRSP rat model compared with the normotensive, insulin-sensitive control strain, Wistar-Kyoto (WKY). We show that skeletal muscle from SHRSP animals exhibits a marked decrease in insulin-stimulated glucose transport compared with WKY animals (fold increase in response to insulin: 1.4 ± 0.15 in SHRSP, 2.29 ± 0.22 in WKY; $n = 4$, $P = 0.02$), but the stimulation of glucose transport in response to activation of AMP-activated protein kinase was similar between the two strains. Similar reductions in insulin-stimulated glucose transport were also evident in myoblast cultures from SHRSP compared with WKY cultures. These differences were not accounted for by a reduction in cellular GLUT4 content. Moreover, analysis of the levels and subcellular distribution of insulin receptor substrates 1 and 2, the p85α subunit of phosphatidylinositol 3′-kinase, and protein kinase B (PKB)/cAKT in skeletal muscle did not identify any differences between the two strains; the insulin-dependent activation of PKB/cAKT was not different between the two strains. However, the total cellular levels of caveolin and flotillin, proteins implicated in insulin signal transduction/compartmentalization, were markedly elevated in skeletal muscles from SHRSP compared with WKY animals. Increased cellular levels of the soluble *N*-ethylmaleimide attachment protein receptor (SNARE) proteins syntaxin 4 and vesicle-associated membrane protein (VAMP)-2 were also observed in the insulin-resistant SHRSP strain. Taken together, these data suggest that the insulin resistance observed in the SHRSP is manifest at the level of skeletal muscle, that muscle cell glucose transport exhibits a blunted response to insulin but unchanged responses to activation of AMP-activated protein kinase, that alterations in key molecules in both GLUT4 trafficking and insulin signal compartmentalization may underlie these defects in insulin action, and that the insulin resistance of these muscles appears to be of genetic origin rather than a paracrine or autocrine effect, since the insulin resistance is also observed in cultured myoblasts over several passages. *Diabetes* 50:2148–2156, 2001

Reduced insulin-stimulated glucose uptake (insulin resistance) by skeletal muscle and adipose tissue is of major pathogenic importance in several common human disorders, including type 2 diabetes, hypertension, obesity, and combined hyperlipidemia, but the underlying mechanisms are unknown (1). The primary nature of the link between insulin resistance and cardiovascular disorders is reinforced by the demonstration that the abnormality is also found in genetic models of hypertension. For example, Reaven et al. (2) showed that the spontaneously hypertensive rat (SHR) exhibited blunted insulin-stimulated glucose transport in adipose tissue compared with control normotensive animals, whereas more recent studies have demonstrated grossly defective insulin inhibition of lipolysis (3). We have recently extended these observations to a close relative of the SHR, the stroke-prone spontaneously hypertensive (SHRSP) rat, and have shown that adipocytes from these animals exhibit blunted insulin-stimulated glucose transport and a reduced ability of insulin to suppress isoproternol-stimulated lipolysis (4). However, although such data clearly show that both SHR and SHRSP exhibit insulin resistance at the cellular level in adipocytes, they provide no information on whether this insulin resistance is also manifest in skeletal muscle, the major site of postprandial glucose disposal (5).

From the [1]Division of Biochemistry and Molecular Biology, University of Glasgow, Glasgow, Scotland; the [2]Department of Medicine and Therapeutics, Western Infirmary, University of Glasgow, Glasgow, Scotland; the [3]Department of Vascular Biology, Glaxo SmithKline, Harlow, U.K.

Address correspondence and reprint requests to Gwyn W. Gould, Division of Biochemistry and Molecular Biology, Davidson Building, University of Glasgow, Glasgow G12 8QQ, Scotland, U.K. E-mail: g.gould@bio.gla.ac.uk.

Received for publication 9 November 2000 and accepted in revised form 13 June 2001.

G.J.M. is employed by and holds stock in SmithKline Beecham. G.W.G. has received an honoraria from SmithKline Beecham.

AICAR, 5-Aminoimidazole-4-carboxamide ribonucleoside; AMPK, AMP-activated protein kinase; deGlc, deoxy-D-glucose; DTT, diothiothreitol; EDL, extensor digitorum longus; eNOS, endothelial nitric oxide synthase; FBS, fetal bovine serum; FDB, flexor digitorum brevis; IRS, insulin receptor substrate; MEM, minimal essential medium; PI3K, phosphatidylinositol 3′-kinase; PKB, protein kinase B; SHR, spontaneously hypertensive rat; SHRSP, stroke-prone spontaneously hypertensive rat; SNARE, soluble *N*-ethylmaleimide attachment protein receptor; VAMP, vesicle-associated membrane protein.

Exercise, like insulin, stimulates glucose disposal via GLUT4 translocation in skeletal muscle (6). However, insulin and exercise appear to promote GLUT4 translocation through distinct intracellular signaling cascades. Thus, in response to insulin, GLUT4 translocation is dependent on the activation of phosphatidylinositol 3′-kinase (PI3K) and is sensitive to the PI3K inhibitor, wortmannin (7). By contrast, exercise-stimulated GLUT4 translocation is wortmannin resistant (7) and appears to involve the activation of AMP-activated protein kinase (AMPK) (8,9). Moreover, these two stimuli appear to act on distinct intracellular pools of GLUT4-containing vesicles (10,11). Several studies have demonstrated defective insulin-stimulated GLUT4 translocation in patients with type 2 diabetes (12–15). By contrast, it is noteworthy that several studies have suggested that normal exercise-stimulated GLUT4 translocation can often be observed in the face of insulin resistance in human type 2 diabetic populations (16–19).

In this report, we show that SHRSP exhibit reduced insulin-stimulated glucose transport in skeletal muscle. Despite this, glucose uptake in response to the activation of AMPK was normal. Furthermore, the insulin resistance of these muscles appears to be of genetic origin rather than a paracrine or autocrine effect because the insulin resistance is also observed in cultured myoblasts. We further show that the insulin resistance in SHRSP muscle does not appear to arise as a consequence of reduced expression of GLUT4, insulin receptor substrate (IRS)-1, IRS-2, PI3K, or protein kinase B (PKB)/cAKT. However, as we observed in another rodent model (the Zucker diabetic fatty rat) (20), elevated levels of expression of the soluble *N*-ethylmaleimide attachment protein receptor (SNARE) proteins, vesicle-associated membrane protein (VAMP)-2, and syntaxin 4 accompanied insulin resistance in skeletal muscle of SHRSP animals. One further phenotype of the SHRSP muscle is that these muscles express markedly elevated levels of caveolin and flotillin. Caveolae have been implicated as potential mediators of the compartmentalization of the insulin signaling cascade (21–23), suggesting that overexpression of caveolin may be an important contributory factor to the insulin resistance observed in the SHRSP. Moreover, flotillin has been implicated as a component of an insulin signaling cascade involved in localizing proteins involved in insulin signal transduction to lipid rafts (21). Hence, the aberrant expression of this protein may have profound functional consequences for the insulin signaling cascade.

RESEARCH DESIGN AND METHODS

Materials. 5-Aminoimidazole-4-carboxamide ribonucleoside (AICAR), cytochalasin B, Pederson Fetuin, collagenase type 1A, and bovine serum albumin fraction V were supplied by Sigma (Poole, U.K.). Hams-F10, α-minimal essential medium (MEM), and fetal bovine serum (FBS) were obtained from Gibco/Life Technologies (Paisley, U.K.). Dr. G. Danielson (Novo Nordisk, Bagsvaerd, Denmark) provided porcine insulin. AMARA peptide (AMARAAS AAALARRR) was a gift from Professor D. G. Hardie, University of Dundee, U.K. PKB substrate peptide (RPRAATF) was from Dr. R. Plevin, University of Strathclyde, U.K. All other reagents were as previously described (20,24,25).

Professor K. Siddle (University of Cambridge) and Dr. E.M. Gibbs (Pfizer, Groton, CT) supplied anti–IRS-1 antibodies. Anti–IRS-2, anti-PKB (PH domain), and anti-p85α antibodies were from Upstate Biotechnologies (TCS Biologicals, Bucks, U.K.). Anti-syntaxin 4 was from Professor D.E. James (University of Queensland) (26), and anti-AMPKα1 and α2 were provided by Prof. D.G. Hardie (University of Dundee) and are described by Woods et al. (27). Anti–endothelial nitric oxide synthase (eNOS) antibodies were from Sigma. Anti–caveolin-1 antibodies were purchased from Becton Dickinson (Oxford, UK). Anti–VAMP-2 antibody was purchased from Synaptic Systems (Gottingen, Germany). Anti-GLUT4 antibody was used as previously described (24). Anti-flotillin antibodies were from Transduction Laboratories (San Diego, CA).

TABLE 1
Characteristics of the animal groups

	n	Blood pressure (mmHg)	Weight (g)
WKY	16	126 ± 11	283.8 ± 26.5
SHRSP	16	174 ± 12*	227.6 ± 13.5*

Data are means ± SE. The SHRSP are known to be smaller in size than age-matched WKY animals (4,28). A statistical difference between the groups is denoted: *$P < 0.02$ for both.

Animals. Male Wistar-Kyoto (WKY) rats and SHRSP rats were reared in house as previously described (4,28). Rats were housed under controlled conditions of temperature (21°C) and light (12-h light-dark cycle) and fed on normal rat diet (rat and mouse no. 1 maintenance diet; Special Diet Services, Edinburgh, U.K.) and water ad libitum. Blood pressure was measured as outlined previously (4,28). Details of the animals are presented in Table 1. Note that differences in body weight in age-matched animals are consistent with previous studies (4,28). Although the SHRSP rats had a slightly smaller body weight than the WKY rats, their muscle weight was slightly increased (Table 1).

Isolation of myoblast cell cultures. Primary skeletal muscle cultures were grown from satellite cells isolated from dissociated muscle tissue by methods adapted from Sarabia et al. (29). Briefly, male rats were killed by CO_2 overdose, and the extensor digitorum longus (EDL) muscle was dissected and cleaned. The muscles from one rat were washed twice in sterile phosphate-buffered saline (room temperature), minced, and enzymatically dissociated by three rounds of mixing at 37°C with 10 ml of 300 units/ml collagenase (type 1A), made up in 0.25% wt/vol trypsin. The supernatant was removed, neutralized with 10% FBS, and centrifuged at 1,000*g* for 5 min. The pellet was resuspended in 4 ml of growth medium (Hams-F10, 20% FBS, 1% penicillin/streptomycin, 1% L-glutamine, 500 mg/l Pederson Fetuin, 500 mg/l BSA, 1 μmol/l dexamethasone, and 1 nmol/l insulin). Resuspended cells were preplated on a noncoated tissue culture flask at 37°C in a 5% CO_2 humidified atmosphere for 2 h, and then the supernatant was transferred to collagen-coated flasks. Cells were fed every third day with growth medium and were passaged once they were 50% confluent. Cells were plated onto collagen-coated plasticware and differentiated when 70–80% confluent by replacing growth medium with differentiation medium (α-MEM, 2% FBS, 1% L-glutamine, 1% penicillin/streptomycin, and 1 nmol/l insulin). Cells were used between 8 and 10 days postdifferentiation.

2-Deoxy-D-glucose transport assays in cultured myoblasts. Serum-starved myoblasts were washed two times in 3 ml of Krebs-Ringer HEPES buffer (118 mmol/l NaCl, 5 mmol/l $NaHCO_3$, 4.7 mmol/l KCl, 1.2 mmol/l KH_2PO_4, 1.2 mmol/l $MgSO_4.7H_2O$, 25 mmol/l HEPES, 2.5 mmol/l $CaCl_2$, pH 7.4) and incubated for 30 min in the presence or absence of 1 nmol/l to 1 μmol/l insulin or 500 μmol/l AICAR (in the presence or absence of 100 nmol/l wortmannin, as indicated in the figure legends). Uptake was initiated by addition of 10 μmol/l 2-deoxy-D-glucose (deGlc) (1 μCi/ml) for 10 min. Specific carrier-mediated deGlc uptake was determined by calculating the cell-associated radioactivity in the presence of 10 μmol/l cytochalasin B. Uptake was stopped by washing in ice-cold phosphate-buffered saline. Cells were lysed in 1 ml of 1% Triton-X100. DeGlc uptake was linear for a period of >30 min under these conditions (data not shown).

2-deGlc transport assays in intact muscle. Flexor digitorum brevis (FDB) muscles were dissected and cleaned of connective tissue without stretching and with tendons intact. Muscles were placed in Krebs-Hensliet buffer (118 mmol/l NaCl, 4.7 mmol/l KCl, 1.2 mmol/l K_2HPO_4, 1.2 mmol/l $MgSO_4.7H_2O$, 25 mmol/l $NaHCO_3$, 2.5 mmol/l $CaCl_2$, pH 7.4, supplemented with 25 mmol/l D-glucose and 0.1% [wt/vol] BSA) and were allowed to recover for 30 min at 37°C with continuous gassing with 95% O_2/5% CO_2. Muscles were pinned at resting length and incubated for 30 min in the presence or absence of 1 μmol/l insulin or 500 μmol/l AICAR; subsequently, the muscles were rapidly washed three times with glucose-free Krebs-Hensliet buffer containing 1% BSA and were incubated for 10 min at 37°C in uptake buffer (Krebs-Hensliet buffer) containing 1 μmol/l insulin, 10 μmol/l deGlc (1 μCi/ml), and [^{14}C]sucrose (0.2 μCi/ml), which was used as an extracellular marker (in the presence or absence of 100 nmol/l wortmannin, as indicated in the figure legends). Muscles were washed three times with ice-cold saline blotted on filter paper and then weighed and solubilized in 1 ml of 0.5N NaOH at 60°C for 45 min, and

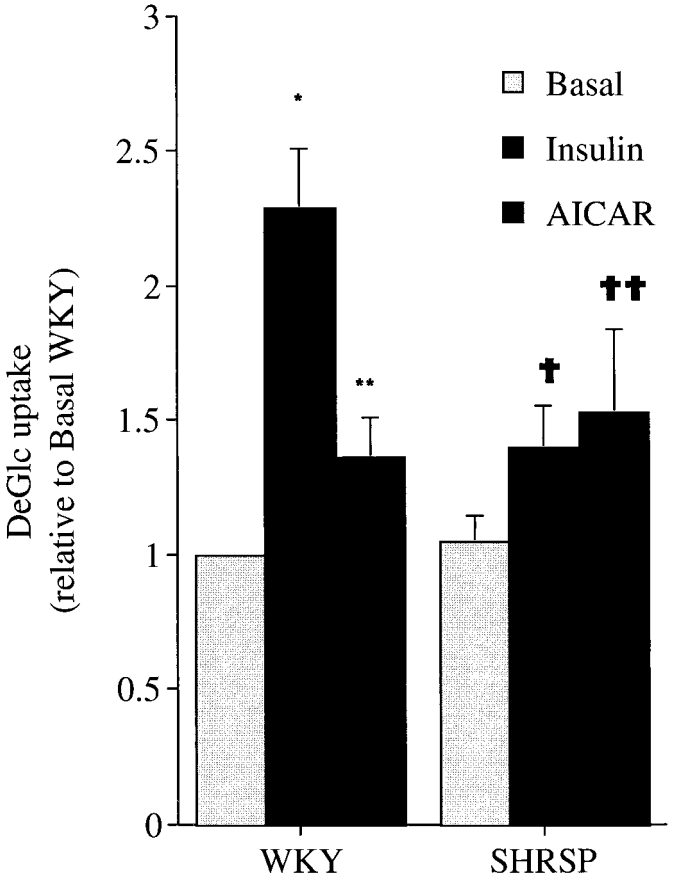

FIG. 1. The effect of insulin and AICAR on deoxyglucose uptake in FDB muscle from SHRSP and WKY muscle. FDB muscles were incubated in Krebs-Hensliet buffer for 30 min in the presence or absence of 1 μmol/l insulin or 500 μmol/l AICAR in 95% air/5% CO_2 before assay of deGlc uptake as previously described. The results are expressed as a fold stimulation over basal (typically between 0.6 and 0.9 pmol · min^{-1} · mg^{-1} wet wt muscle). Basal rates were not significantly different between the two strains. The results shown are the means ± SE for four experiments. A statistically significant increase in response to insulin (*P = 0.02) and a significant increase in response to AICAR (P = 0.05) are indicated. †Indicates a significant increase in response to insulin compared with SHRSP basal (P < 0.05) and that the magnitude of the insulin response is lower in SHRSP compared with WKY muscles (P = 0.02); †† indicates a statistically significant increase in response to AICAR (P = 0.03) and refers to no significant difference in the magnitude of the AICAR effects between the two strains. The average wet weight of muscle from these animals was 45.7 ± 4.8 mg (WKY) and 61.1 ± 11.6 mg (SHRSP) (n = 16 individual muscles).**

tissue-associated radioactivity was determined. In control studies, we have found that the uptake of deGlc is linear for at least 20 min under these conditions in both SHRSP and WKY FDB muscle (data not shown).

Preparation of muscle extracts. Freshly dissected muscles were homogenized using a Polytron in ice-cold lysis buffer (50 mmol/l HEPES pH7.4, 1% NP40, 150 mmol/l NaCl, 5 mmol/l $Na_4P_2O_7$, 5 mmol/l Na_3VO_4, 1 mmol/l EDTA, 1 mmol/l EGTA, 1 mmol/l diothiothreitol (DTT), 10% glycerol, and protease inhibitors), followed by 20 strokes in a Dounce homogenizer. The homogenate was centrifuged at 14,000*g* for 5 min at 4°C to remove unsolubilized material. Aliquots of the solubilized protein were analyzed by immunoblotting as described below. Note that this procedure is sufficient to solubilize >95% of the cellular caveolin and flotillin (data not shown).

Fractionation of skeletal muscle. Muscles were isolated and snap frozen. Frozen tissue was powdered on dry ice and resuspended in HES buffer (20 mmol/l HEPES, pH 7.4, 1 mmol/l EDTA, 250 mmol/l sucrose, 2 mmol/l sodium orthovanadate, 10 mmol/l NaF, and 1 mmol/l sodium pyrophosphate), supplemented with proteinase inhibitor tablets (Boehringer Mannheim), before homogenization. The homogenate was centrifuged at 12,000*g* for 20 min at 4°C and the pellet was collected (heavy membrane fraction). The supernatant was further centrifuged at 140,000*g* for 1 h at 4°C, and the pellet (light membrane fraction) and supernatant (soluble protein fraction) were collected. These fractions were assayed for protein and resuspended in SDS-PAGE sample buffer before immunoblot analysis.

PKB/cAKT assays. Muscles were isolated by dissection, placed in Krebs-Hensliet buffer supplemented with 25 mmol/l D-glucose and 0.1% (wt/vol) BSA, and allowed to recover for 30 min at 37°C with continuous gassing with 95% O_2/5% CO_2. Muscles were incubated for 30 min in the presence or absence of 1 μmol/l insulin, after which the muscles were rapidly washed three times with glucose-free Krebs-Hensliet buffer and snap frozen. Frozen tissue was powdered using a mortar and pestle on dry ice and resuspended in lysis buffer (50 mmol/l Tris-HCl pH 7.4, 50 mmol/l NaF, 1 mmol/l sodium pyrophosphate, 1 mmol/l EDTA, 1 mmol/l EGTA, 50 mmol/l mannitol, 1 mmol/l DTT, 0.1 mmol/l benzamidine, 0.1 mmol/l phenylmethylsulfonyl fluoride, 1 mmol/l Na_3VO_4, 5 μg/ml soybean trypsin inhibitor, and 1% Triton X-100). Muscle lysates were spun in a microfuge at 14,000 rpm for 10 min to remove insoluble material. PKB immunoprecipitation and assay were carried out using triplicate samples (200 μg) of soluble muscle lysate, exactly as described by Salt et al. (25).

Immunoblot analysis. Protein samples were separated on SDS-PAGE and transferred to nitrocellulose, as outlined by Maier et al. (20). Immuno-labeled proteins were visualized using horseradish-peroxidase–conjugated secondary antibody and the enhanced chemiluminescence system (Amersham, Amersham, U.K.). Bands were quantified by densitometry using a BioRad GS700 system. To quantify the relative levels of expression, increasing loads of protein were loaded into adjacent lanes, and the linearity of the immunoblot signal was determined by densitometric analysis of blots developed using enhanced chemiluminescence. Multiple exposures of X-ray film were performed to insure linearity of response to film to signal. All immunoblot signals were quantified from linear regions of the protein titration curve, as outlined by Maier et al. (20).

Statistical analysis. Statistical analysis was performed using Student's t test with StatView software (Abacus, Stanford, CA). $P \leq 0.05$ was taken as a significant difference between groups.

RESULTS

The characteristics of the animals used in this study are shown in Table 1. Blood pressure was higher in the SHRSP compared with the WKY animals. We have previously shown that adipocytes from these animals exhibit reduced insulin-stimulated glucose transport in isolated adipocytes and a blunted ability of insulin to suppress isoproternol-stimulated lipolysis compared with the isogenic WKY strain (4). We therefore examined the ability of insulin to stimulate deGlc uptake in isolated FDB muscle from these animals. Figure 1 compares the response to insulin and AICAR, an activator of AMPK, on deGlc transport. As shown, muscles from SHRSP exhibit decreased insulin-stimulated deGlc uptake compared with WKY muscles, but the response to AICAR is essentially identical between the two groups. Consistent with other studies, wortmannin (100 nmol/l) completely blocked insulin-stimulated deGlc transport but was without effect on AICAR-stimulated glucose transport (data not shown).

The stimulation of glucose transport in skeletal muscle is mediated by the GLUT4 glucose transporter (10). We

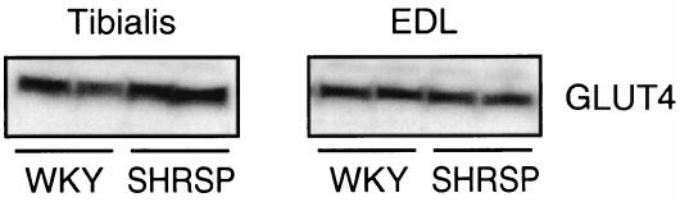

FIG. 2. Immunoblot analysis of GLUT4 levels in muscle from SHRSP and WKY animals. Shown is a representative immunoblot for GLUT4 levels in either tibialis or EDL muscles from SHRSP or WKY animals in which 20 μg of muscle lysate was loaded per lane. Shown are samples from two different animals. Quantification of GLUT4 protein levels in these muscles from six different animals revealed no significant differences between the two strains (data not shown).

therefore determined the total cellular levels of GLUT4 in skeletal muscle membranes from SHRSP and WKY animals by quantitative immunoblotting. Figure 2 demonstrates that GLUT4 levels are similar in different muscles from SHRSP and WKY animals. These data indicate that reduced GLUT4 expression cannot explain the reduced ability of insulin to stimulate deGlc uptake in SHRSP muscle.

In an attempt to identify differences between the SHRSP and WKY muscle that could account for the observed insulin resistance, we have characterized the cellular content and distributions of proteins involved in insulin signaling and GLUT4 trafficking in muscles of these animals. Figure 3 shows an immunoblot analysis of the levels and distribution of IRS-1, IRS-2, and the p85α subunit of PI3K in muscle fractions. We have compared the levels of these proteins in three crude subcellular fractions of muscle, specifically a heavy membrane fraction, a light membrane fraction (enriched in intracellular membranes, as evidenced by the majority of cellular GLUT4 being present in this fraction), and a soluble protein fraction (Fig. 3). As has been reported in adipocytes (30–32), these key insulin signaling molecules are localized predominantly in the light membrane and soluble protein fractions of muscle. Neither the absolute level nor the distribution among these fractions was significantly different between SHRSP and WKY animals (Figs. 3 and 5). Hence, it would seem unlikely that defective expression of IRS-1, IRS-2, or PI3K can explain the insulin resistance observed in SHRSP muscles.

To further evaluate possible signaling defects associated with insulin action in these muscles, we assayed the ability of insulin to stimulate PKB activity in these muscles because PKB has been suggested to be involved in the insulin-stimulated translocation of GLUT4 to the plasma membrane of both adipocytes and muscle (33–37). The result of this analysis is shown in Fig. 4. No differences in the basal or insulin-stimulated PKB activity were observed in soleus or EDL muscles isolated from SHRSP and WKY animals.

Figure 5 shows an immunoblot analysis in which we compared the total cellular content of VAMP2, VAMP3/cellubrevin, and syntaxin 4, which are the SNARE proteins that mediate GLUT4 translocation (38) in total muscle extracts. Quantification of these data revealed that VAMP2 expression was elevated 1.9 ± 0.2–fold in EDL and 1.7 ± 0.3–fold in tibialis muscles from the insulin-resistant SHRSP strain compared with WKY animals ($P = 0.02$ for both). VAMP3/cellubrevin levels were also raised in both muscles (53% in EDL and 1.5 ± 0.13–fold in tibialis), but this increase only reached statistical significance in the tibialis muscle ($P < 0.05$). Syntaxin 4 levels were also increased in EDL (1.08 ± 0.2–fold, $P = 0.03$) and tibialis (1.8 ± 0.05–fold, $P = 0.02$) muscles from SHRSP animals. By contrast, cellular levels of AMPKα2, PKB/cAKT, and eNOS did not differ significantly between strains in either muscle (Fig. 4). AMPKα1 was barely detectable in these tissues, consistent with published results (data not shown) (39).

Recent studies have implicated caveolae and/or lipid rafts as possible components of the insulin signaling apparatus. We therefore examined the level of expression of caveolin isoforms in muscle tissue from SHRSP and WKY animals, as well as the expression of flotillin, a protein known to be enriched in membrane rafts and one

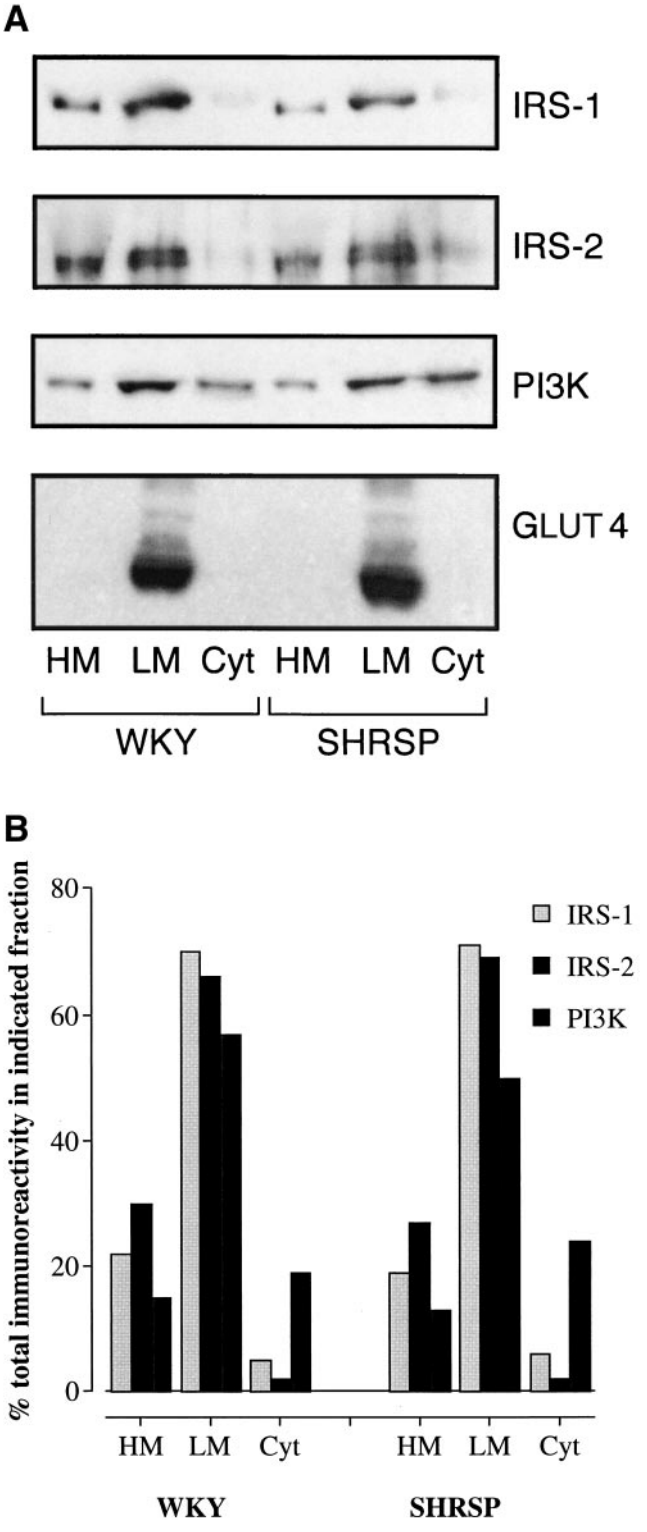

FIG. 3. Immunoblot analysis of insulin signaling proteins in skeletal muscle from SHRSP and WKY rats. The distribution of IRS-1, IRS-2, and the p85α subunit of PI3K in skeletal muscle fractions from SHRSP and WKY animals was analyzed by quantitative immunoblotting (*A*). The light membrane (LM) fraction contains the majority of the intracellular membranes, as evidenced by the majority of the cellular GLUT4 being present in this fraction. Cyt, soluble protein fraction; HM, heavy membranes. The data presented are representative of four separate experiments of this type in which 20 μg of each fraction was loaded on each lane of the gel. No significant differences in either expression level of subcellular distribution were observed for any of the proteins studied. *B*: Quantification of four experiments of this type in which the distribution of these molecules among the different fractions is presented, expressed as a percentage of total immunoreactivity (means ± SE).

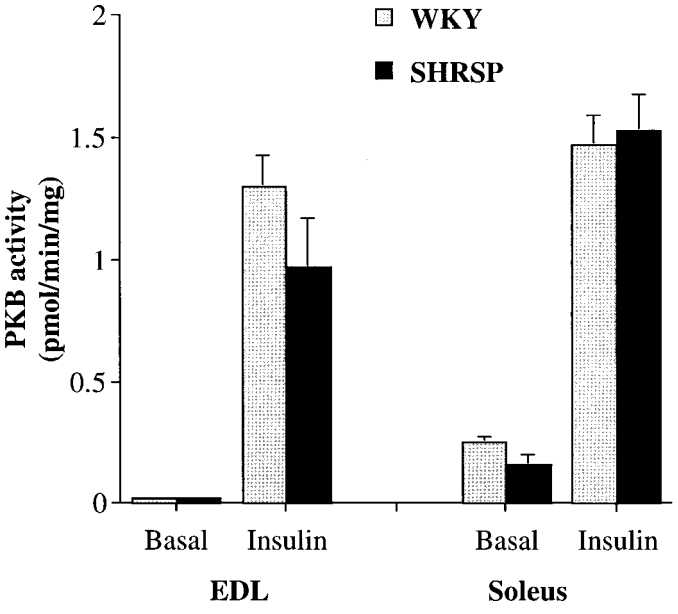

FIG. 4. PKB activity in muscles. EDL or soleus muscles were incubated with or without 1 mmol/l insulin for 30 min, and PKB/cAKT activity was determined as previously outlined. Shown is data from three experiments (means ± SE), with each condition performed in triplicate in each experiment. No significant differences were observed between the strains.

that has been implicated as a component of the insulin signaling cascade. The results are shown in Fig. 6. Levels of expression of caveolin-1 and flotillin were found to be markedly elevated in SHRSP compared with controls. Caveolin expression was increased in EDL muscle by 2.4 ± 0.4–fold ($P = 0.005$) and in tibialis by 3.34 ± 0.4–fold ($P = 0.002$). Similarly, flotillin levels were also increased by 1.9 ± 0.05–fold and 1.7 ± 0.12–fold in EDL and tibialis muscles, respectively ($P < 0.05$ for both).

It is possible that the insulin resistance observed in SHRSP may be secondary to changes in physiology, such as altered blood flow to the muscle beds by defective vasodilatation in response to insulin or by changes in circulating factors that regulate peripheral insulin sensitivity. To address this, we isolated myoblast cultures from muscle satellite cells isolated from SHRSP or WKY animals. These multinucleated cells exhibited high levels of expression of the muscle-specific markers MyoD, myogenin desmin, and sarcomeric-α-actin (data not shown). We therefore examined the ability of insulin and AICAR to stimulate deGlc uptake in these cells. Figure 7*A* shows a typical dose response of deGlc uptake to insulin. We routinely observed both a decreased maximal rate of insulin-stimulated deGlc uptake and a rightward shift of the dose-response curve in myoblasts from SHRSP compared with WKY animals. Figure 7*B* demonstrates that myoblast cell cultures from SHRSP muscle exhibit blunted insulin-stimulated deGlc uptake compared with WKY, but the response to AICAR was similar between the two cultures. Consistent with data on intact muscle, pretreatment with 100 nmol/l wortmannin completely blocked insulin-stimulated deGlc uptake but was without effect on AICAR-stimulated deGlc uptake.

DISCUSSION

Glucose transport in skeletal muscle is stimulated by both insulin and exercise. Insulin-stimulated glucose transport

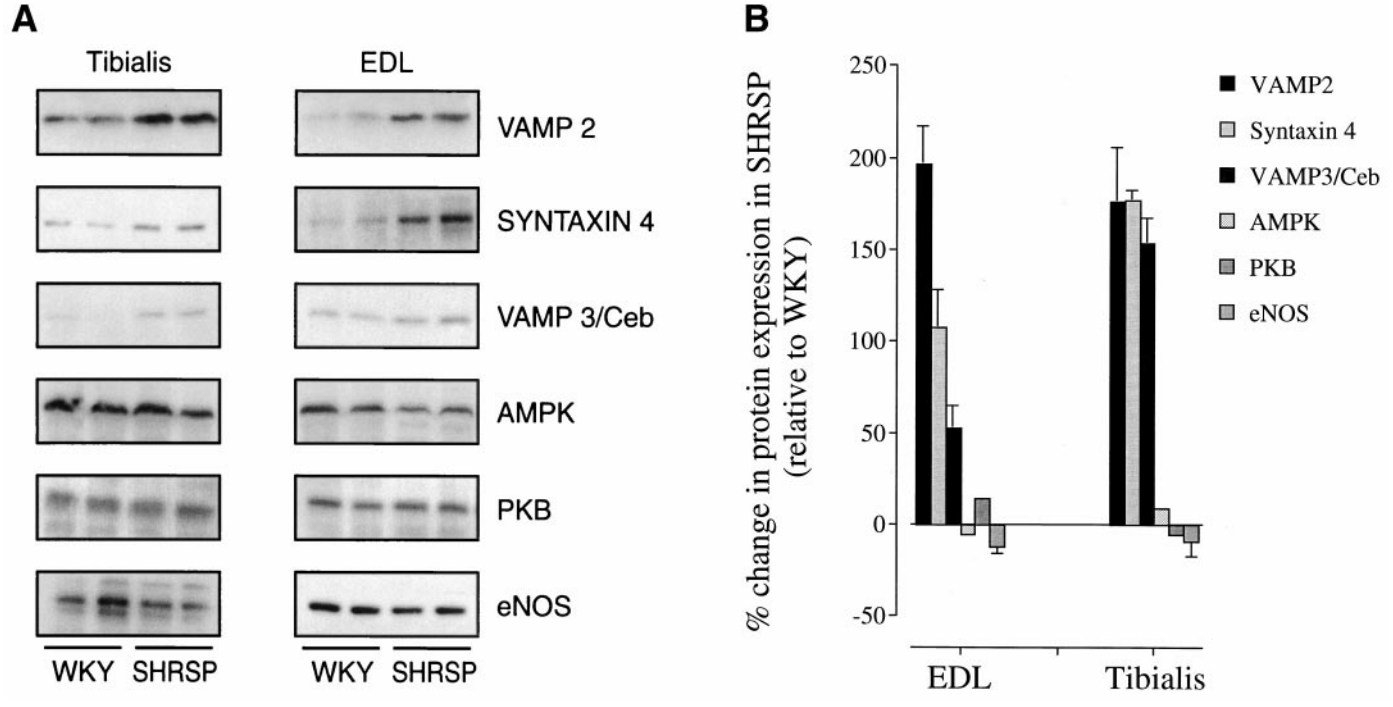

FIG. 5. Immunoblot analysis of SNARE proteins in skeletal muscle from SHRSP and WKY rats. Shown are representative immunoblots (*A*) in which 20 μg of protein lysates made from the skeletal muscle of male SHRSP or WKY animals were analyzed by SDS-PAGE/immunoblotting with the antibodies. *B*: Quantification of four experiments of this type, with the relative level of expression in SHRSP muscle expressed as a percent of that observed in the corresponding WKY muscle (means ± SE). Data from two separate experiments are shown for each of the EDL and tibialis muscles. Results obtained using antibodies specific for eNOS, AMPKα2, and PKB-PH are shown to illustrate that the observed changes in SNARE protein expression are not a consequence of global increases in the expression of proteins implicated in insulin or exercise signal transduction. Details of statistically significant differences are not presented on the graph for clarity but are included in the text.

is reduced in type 2 diabetes and insulin resistance, but several studies have suggested that exercise-stimulated glucose transport is unaffected in such individuals (17–19,40). Understanding the molecular basis for defective insulin action is of fundamental importance, given the greatly increased incidence of cardiovascular disease in individuals with type 2 diabetes (41,42). In this study, we have examined the ability of insulin and AICAR (an activator of AMPK) to modulate glucose transport in skeletal muscle from SHRSP compared with the normotensive, insulin-sensitive WKY strain. We have shown that muscle from SHRSP exhibits blunted insulin-stimulated glucose transport (Fig. 1), and these data are in agreement with our previous observation that adipocytes from these animals also exhibit defective insulin action (4).

AMPK is activated in response to exercise in both human and rodent muscle (8,9). AMPK has therefore been suggested to play a crucial role in exercise-stimulated glucose transport, based on studies showing that treatment of muscle with AICAR can activate glucose transport by a mechanism similar to that induced by exercise (8,9). Strikingly, AICAR is able to activate glucose transport to a similar extent in muscle from both SHRSP and WKY strains (Fig. 1), suggesting that the insulin resistance observed in the SHRSP is confined to an insulin-specific step in the activation of glucose transport. This step is not due to aberrant expression of the major insulin-responsive glucose transporter, GLUT4, because levels of expression of this protein were found to be similar in all muscles examined (EDL, tibialis, and FDB) (Fig. 2).

To further address the mechanism of the observed insulin resistance, we isolated myoblast cultures from SHRSP and WKY animals. These cultures exhibited high levels of expression of a range of skeletal muscle markers and expressed GLUT4 (data not shown). Like intact muscle, these cultures exhibit insulin- and AICAR-stimulated glucose transport (Fig. 7). Remarkably, the defect observed in insulin-stimulated glucose transport in intact muscles from the SHRSP was also observed in myoblast cultures (Fig. 7*B*). We have found that this diminution of insulin sensitivity was evident throughout all passages of the cells (we have examined up to passage 7). These data strongly argue that the defect observed in isolated muscle strips is an inherent genetic defect and does not reflect an adaptive response of the muscle to altered blood flow or circulating factors.

In an attempt to identify possible sites of lesion in the insulin signaling cascade, we have examined the levels of expression and subcellular localization and activity of several key proteins implicated in insulin-stimulated glucose transport, specifically IRS-1, IRS-2, and PI3K (Figs. 3–5) (43,44). The subcellular distribution of IRS-1 and IRS-2 is modulated by insulin (44). The association of IRS-1 with a cytoskeletal 'scaffold' adjacent to the plasma membrane has been suggested to be a fundamental aspect of insulin signaling in adipocytes (30). In response to insulin treatment, IRS-1 is released from this scaffold and appears to behave as a soluble protein, moving from the particulate to the cytosolic fraction upon subcellular analysis (30). In an effort to address whether IRS proteins were cytosolic or particulate in muscle, we subjected muscle homogenates to subcellular fractionation. Analysis of the

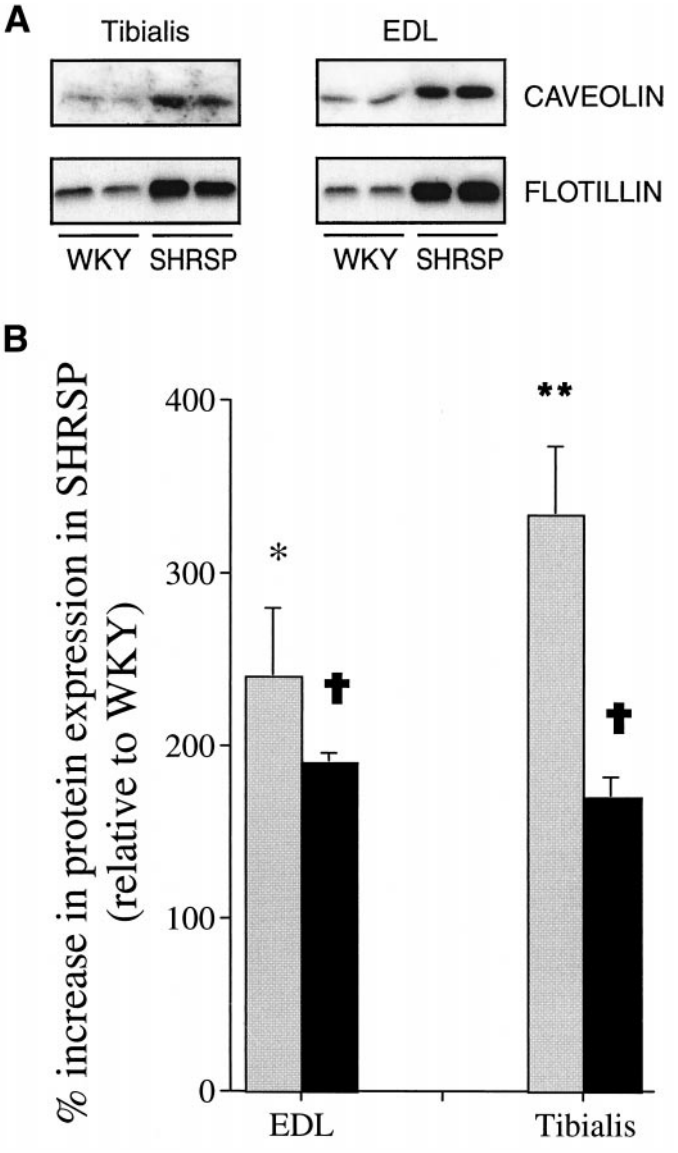

FIG. 6. Immunoblot analysis of caveolin and flotillin in skeletal muscle from SHRSP and WKY rats. Shown are representative immunoblots (*A*) in which 20 μg of protein lysates made from skeletal muscle of male SHRSP or WKY animals were analyzed by SDS-PAGE/immunoblotting with the antibodies indicated. Data from two separate animals of each strain are shown; note that the blots presented are deliberately overexposed to show the level of caveolin (▨) and flotillin (■) present in WKY animals. *B*: Quantification of four experiments of this type, with the relative level of expression in SHRSP muscles expressed as a percent of that observed in the corresponding WKY muscle (means ± SE). Statistically significant increases in SHRSP compared with WKY are indicated: **P* = 0.005, ***P* = 0.002, †*P* < 0.05.

subcellular distribution of IRS-1 and IRS-2 revealed that these molecules were associated with both heavy and light membrane fractions, with some immunoreactivity evident in the cytosolic fraction (Fig. 3). However, comparison of these fractions from SHRSP and WKY strains revealed no differences in either total level of expression or subcellular distribution (Fig. 3). Hence, it would appear unlikely that the primary defect in insulin action in the SHRSP lies at the level of expression or localization of these proteins. Similarly, levels of expression of AMPKα2 (the major isoform in skeletal muscle) (39) and both α- and β-isoforms of PKB/cAKT and eNOS were similar between the two groups (Fig. 5).

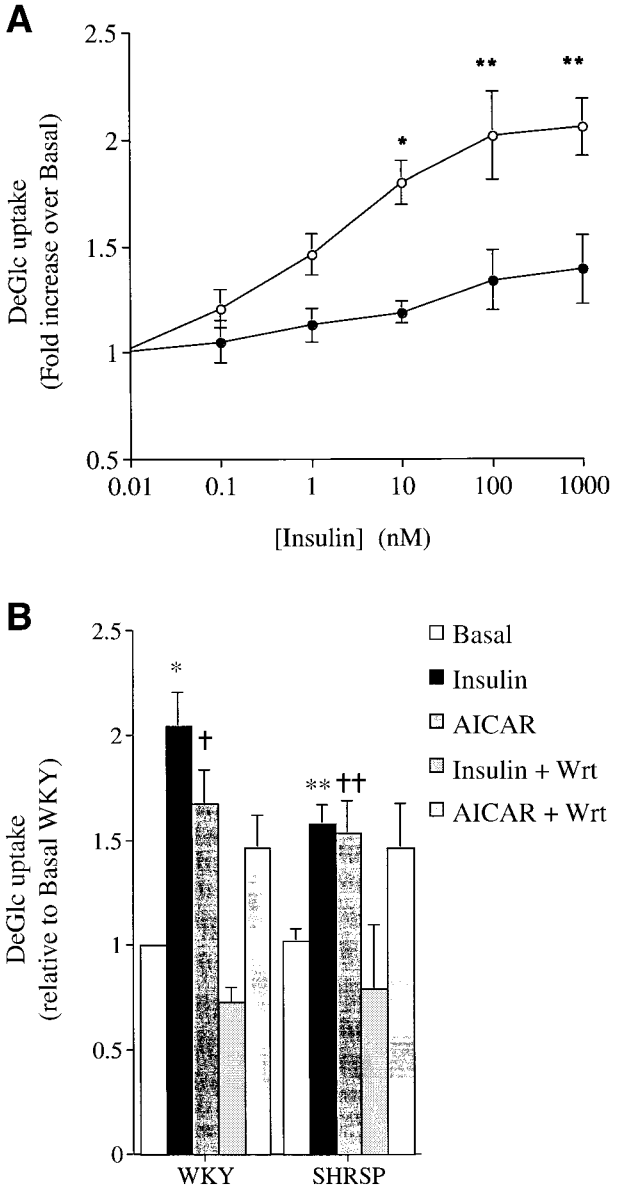

FIG. 7. DeGlc uptake in cultured myoblasts. The effects of insulin, AICAR, and wortmannin. *A*: A typical dose-response curve for insulin in cultured myoblasts from SHRSP (●) or WKY (○) strains. Serum-starved myoblast were washed two times in Krebs-Ringer HEPES buffer, and then incubated in Krebs-Ringer HEPES for 30 min in the presence or absence of the indicated concentration of insulin. Each point is the mean of triplicate determinations and is corrected for the nonspecific association of deGlc uptake with the cells. Data from a representative experiment are shown, expressed as a fold increase relative to basal WKY–derived cultures. A significant difference between SHRSP and WKY points is illustrated by *P = 0.05 and **P = 0.01. The experiment was repeated five times with similar results. The basal rates of transport were not significantly different between WKY- and SHRSP- derived cultures. *B*: The effects of a 30-min incubation with either 1 mmol/l insulin or 500 mmol/l AICAR on deGlc uptake. The effect of pretreatment of the cells with 100 nmol/l wortmannin on these stimulations is also shown. Data are means ± SE from three separate experiments, expressed as a fold increase over the basal WKY rate. A significant increase in transport in response to insulin (*P = 0.01), a significant reduction in insulin-stimulated glucose transport compared with WKY strain (P = 0.04), and a significant increase in response to AICAR in WKY cultures (†P = 0.05) are indicated. ††Indicates no significant difference in the magnitude of the AICAR response between the WKY and SHRSP strains and that the AICAR response in SHRSP cultures is significantly increased over basal (P = 0.05). Wortmannin-inhibited insulin stimulated deGlc uptake significantly in both WKY and SHRSP cultures (P = 0.01) and had no significant effect on AICAR-stimulated deGlc transport. Symbols are omitted from the graph for clarity.**

In an effort to address whether the extent of activation of downstream signaling molecules differed between the two strains, we assayed PKB/cAKT activity in both soleus and EDL muscles from SHRSP and WKY animals. As shown in Fig. 4, no difference in either basal or insulin-stimulated PKB activity was observed between these strains. These data suggest that the defect in insulin action observed in the insulin-resistant SHRSP is not a consequence of defective activation of this important kinase.

We next turned our attention to other molecules involved in the translocation of GLUT4, particularly the SNARE proteins, in which some notable differences were observed between the two strains (Fig. 5). Firstly, we observed elevated expression of VAMP2 and syntaxin 4 in the insulin-resistant SHRSP muscle compared with control animals. Insulin-stimulated GLUT4 translocation represents a highly regulated vectorial delivery of defined intracellular cargo to the plasma membrane. The fidelity of this response is mediated at least in part by SNARE proteins (38,45). Studies have identified homologs of SNAREs in adipocytes and muscle, in particular syntaxin 4 and VAMP2. GST-fusion proteins for each of these SNARE proteins inhibit insulin-stimulated GLUT4 translocation in muscle and fat cells, arguing cogently for a crucial functional role of these proteins in insulin action (24,26,46–51). We have shown that VAMP2 and syntaxin 4 SNARE protein expression is significantly upregulated in the insulin-resistant Zucker diabetic fatty rat (20). Similar data were observed in the present study; VAMP2 expression was doubled in both EDL and tibialis muscle from SHRSP compared with WKY ($P < 0.01$), and syntaxin 4 levels were also increased. Such data suggest that upregulation of SNARE proteins may be evident in a range of insulin-resistant models. However, whether these changes are causal or adaptive remains to be determined. Interestingly, elevated levels of both VAMP2 and syntaxin 4 were also observed in isolated myoblast cultures from SHRSP compared with WKY animals (data not shown). Such observations could suggest that the overexpression of SNARE proteins may be more than simply an adaptive change to whole-animal insulin sensitivity. However, further work will be required to address this issue.

One other major difference between these two strains was identified in this study. Specifically, the expression of caveolin and flotillin were markedly elevated in muscle from the insulin-resistant SHRSP compared with WKY animals (Fig. 6). Caveolin is the major structural protein of caveolae, which are flask-like invaginations of the cell surface (52). Caveolae have been implicated as components of the spatial organization of intracellular signaling cascades, and several studies have reported localization of insulin receptors to these structures (21–23,53). Caveolin expression is induced upon differentiation of adipocytes (54), and insulin stimulates tyrosine phosphorylation of caveolin in fat cells (23). More recently, the localization of insulin-regulated CAP proteins to caveolae has argued strongly for an important (but as yet undefined) role for caveolae in insulin signal transduction (21,55). The overexpression of caveolin observed in skeletal muscle of the SHRSP strain may therefore be an important contributory factor to the insulin resistance observed in these animals. Whether increased expression of caveolin could result in

the sequestration of important insulin signaling components in an inactive environment or act as an inhibitor of downstream effects remains to be determined. Strikingly, the lipid raft–associated protein, flotillin, is also markedly overexpressed in SHRSP muscles compared with WKY. Flotillin has been proposed to localize a protein complex of CAP-Cbl proteins to lipid rafts in adipocytes that may play a crucial role in propagation of the insulin signal, at least in adipocytes (21). The fact that both caveolin and flotillin are overexpressed in muscle from the SHRSP suggests that overexpression of caveolae-associated proteins may act to blunt the ability of insulin receptors to signal to proximal molecules in the insulin signaling cascade. Further studies will be required to test this hypothesis in a systematic fashion. It is interesting to note that caveolin and flotillin were overexpressed in myoblast cultures from SHRSP animals compared with WKY cultures by similar magnitudes (data not shown).

In summary, we have shown that skeletal muscle of SHRSP exhibits reduced insulin-stimulated glucose transport compared with WKY isogenic controls. However, the response to activation of AICAR was indistinguishable between the two strains, suggesting that the defect in insulin action lies on a specific arm of the machinery or signaling cascade activated by insulin. We further show that SHRSP, like the insulin-resistant Zucker diabetic fatty rat, exhibits elevated VAMP2 and syntaxin 4 expression in skeletal muscle, suggesting that this defect may be common to a range of rodent models of insulin resistance. Finally, we report for the first time that caveolin and flotillin are overexpressed in the insulin-resistant muscles. This result may be of considerable importance, given the proposed central role of caveolae in the organization of the insulin signaling system.

ACKNOWLEDGMENTS

This work was supported by the Medical Research Council (MRC) (Cooperative Group Grant G9800025 and Component Grant G9901492 to J.M.C.C., A.F.D., and G.W.G.), the Wellcome Trust (equipment grant to G.W.G.), the British Heart Foundation (project grant to G.W.G. and A.F.D., and a fellowship to I.P.S.), and the University of Glasgow (J.M.C.C. and G.W.G.). D.J.J. is supported by a Collaborative Awards in Science and Engineering PhD studentship with Glaxo SmithKline. The authors are grateful to S.J. Yeaman and D. Turnbull (University of Newcastle) for help in establishing myoblast cultures and to all colleagues who generously supplied reagents and advice during this study.

REFERENCES

1. Reaven GM: Banting Lecture 1988: Role of insulin resistance in human disease. *Diabetes* 37:1595–1607, 1988
2. Reaven GM, Chang H, Hoffman BB, Azhar S: Resistance to insulin-stimulated glucose uptake in adipocytes isolated from spontaneously hypertensive rats. *Diabetes* 38:1155–1160, 1989
3. Aitman TJ, Glazier AM, Wallace CA, Cooper LD, Norsworthy PJ, Wahid FN, Al-Majali KM, Trembling PM, Mann CJ, Shoulders CC, Graf D, St Lezin E, Kurtz TW, Kren V, Pravenec M, Ibrahimi A, Abumrad NA, Stanton LW, Scott J: Identification of Cd36 (Fat) as an insulin-resistance gene causing defective fatty acid and glucose metabolism in hypertensive rats. *Nat Genet* 21:76–83, 1999
4. Collison M, Glazier AM, Aitman TJ, Scott J, Graham D, Morton JJ, Dominiczak MH, Connell JMC, Gould GW, Dominiczak AF: *Cd36* and molecular mechanisms on insulin resistance in the stroke-prone spontaneously hypertensive rat. *Diabetes* 49:2222–2226, 2000
5. James DE, Burleigh KM, Kraegen EW: In vivo glucose metabolism in individual tissues of the rat. *J Biol Chem* 261:6366–6374, 1986
6. Zorzano A, Munoz P, Camps M, Mora C, Testar X, Palacin M: Insulin-induced redistribution of GLUT4 glucose carriers in the muscle fiber: in search of GLUT4 trafficking pathways. *Diabetes* 45: S70–S81, 1996
7. Yeh JI, Gulve EA, Rameh L, Birnbaum MJ: The effects of wortmannin on rat skeletal muscle: dissociation of signalling pathways for insulin- and contraction-activated hexose transport. *J Biol Chem* 270:2107–2111, 1995
8. Hayashi T, Hirshman MF, Kurth EJ, Winder WW, Goodyear LJ: Evidence for 5′AMP-activated protein kinase mediation of the effect of muscle contraction on glucose transport. *Diabetes* 47:1369–1373, 1998
9. Kurth-Kracznek EJ, Hirshmann MF, Goodyear LJ, Winder WW: 5′ AMP-activated protein kinase activation causes GLUT4 translocation in skeletal muscle. *Diabetes* 48:1667–1671, 1999
10. Ploug T, van Deurs B, Ai H, Cushman SW, Ralston E: Analysis of GLUT4 distribution in whole skeletal muscle fibers: identification of distinct storage compartments that are recruited by insulin and muscle contractions. *J Cell Biol* 142:1429–1446, 1998
11. Aledo JC, Lavoie L, Volchuck A, Keller SR, Klip A, Hundal HS: Identification and characterization of two distinct intracellular GLUT4 pools in rat skeletal muscle: evidence for an endosomal and an insulin-sensitive GLUT4 compartment. *Biochem J* 325:727–732, 1997
12. Kahn BB, Rosen AS, Bak JF, Andersen PH, Damsbo P, Lund S, Pedersen O: Expression of GLUT1 and GLUT4 glucose transporters in skeletal muscle of humans with insulin-dependent diabetes mellitus: regulatory effects of metabolic factors. *J Clin Endocrinol Metab* 74:1101–1109, 1992
13. Kahn BB: Alterations in glucose transporter expression and function in diabetes: mechanisms for insulin resistance. *J Cell Biochem* 48:122–128, 1992
14. Garvey WT, Maianu L, Hancock JA, Golichowski AM, Baron A: Gene expression of GLUT4 in skeletal muscle from insulin-resistant patients with obesity, IGT, GDM and NIDDM. *Diabetes* 41:465–475, 1992
15. Garvey WT, Maianu L, Zhu J-H, Brechtel-Hook G, Wallace P, Baron AD: Evidence for defects in the trafficking and translocation of GLUT4 glucose transporters in skeletal muscle as a cause of human insulin resistance. *J Clin Invest* 101:2377–2386, 1998
16. Goodyear LJ, Hirshman MF, Horton ES: Exercise-induced translocation of skeletal muscle glucose transporters. *Am J Physiol* 261:E795–E799, 1991
17. Hughes VA, Fiatarone MA, Fielding RA, Kahn BB, Ferrara CM, Shepherd P, Fisher EC, Wolfe RR, Elahi D, Evans WJ: Exercise increases muscle GLUT-4 levels and insulin action in subjects with impaired glucose tolerance. *Am J Physiol* 264: E855–E862, 1993
18. Kennedy JW, Hirshman MF, Gervino EV, Ocel JV, Forse RA, Hoenig SJ, Aronson D, Goodyear LJ, Horton ES: Acute exercise induces GLUT4 translocation in skeletal muscle of normal human subjects and subjects with type 2 diabetes. *Diabetes* 48:1192–1197, 1999
19. Wojtaszewski JFP, Hansen BF, Gade J, Kiens B, Markuns JF, Goodyear LJ, Richter EA: Insulin signaling and insulin sensitivity after exercise in human skeletal muscle. *Diabetes* 49:325–331, 2000
20. Maier V, Melvin DR, Lister CA, Chapman H, Gould GW, Murphy GJ: v- and t-SNARE protein expression in models of insulin resistance: normalization of glycemia by rosiglitazone treatment corrects overexpression of cellubrevin, vesicle-associated membrane protein-2, and syntaxin 4 in skeletal muscle of Zucker diabetic fatty rats. *Diabetes* 49:618–625, 2000
21. Baumann CA, Ribon V, Kanzaki M, Thurmond DC, Mora S, Shigematsu S, Bickel PE, Pessin JE, Saltiel AR: CAP defines a second insulin signalling pathway required for insulin-stimulated glucose transport. *Nature* 407: 202–207, 2000
22. Mastick CC, Brady MJ, Saltiel AR: Insulin stimulates the tyrosine phosphorylation of caveolin. *J Cell Biol* 129:1523–1531, 1995
23. Mastick CC, Saltiel AR: Insulin-stimulated tyrosine phosphorylation of caveolin is specific for the differentiated adipocyte phenotype in 3T3–L1 adipocytes. *J Biol Chem* 272:20706–20714, 1997
24. Millar CA, Sherwan A, Hickson GRX, James DE, Gould GW: Differential regulation of secretory compartments containing the insulin-responsive glucose transporter, GLUT4, in 3T3–L1 adipocytes. *Mol Biol Cell* 10:3675–3688, 1999
25. Salt IP, Connell JMC, Gould GW: 5-Aminoimidazole-4-carboxamide ribonucleoside (AICAR) inhibits insulin-stimulated glucose transport in 3T3–L1 adipocytes. *Diabetes* 49:1649–1656, 2000
26. Tellam JT, Macaulay SL, McIntosh S, Hewish DR, Ward CW, James DE: Characterization of Munc-18c and syntaxin-4 in 3T3–L1 adipocytes: putative role in insulin-dependent movement of GLUT-4. *J Biol Chem* 272: 6179–6186, 1997

27. Woods A, Salt IP, Scott JD, Hardie DG, Carling D: The α1 and α2 isoforms of the AMP-activated protein kinase have similar activities in rat liver but exhibit differences in substrate specificity in vitro. *FEBS Lett* 397:347–351, 1996
28. Jeffs B, Clark JS, Anderson NH, Gratton J, Brosnan MJ, Gauguier D, Reid JL, Macrae IM, Dominiczak AF: Sensitivity to cerebral ischaemic insult in a rat model of stroke is determined by a single genetic locus. *Nat Genet* 16:364–367, 1997
29. Sarabia V, Lam L, Burdett E, Leiter LA, Klip A: Glucose transport in human skeletal muscle cells in culture: stimulation by insulin and metformin. *J Clin Invest* 90:1386–1395, 1992
30. Clark SF, Martin S, Carozzi AJ, Hill MM, James DE: Intracellular localisation of phosphatidylinositide 3-kinase and insulin receptor substrate-1 in adipocytes: potential involvement of a membrane skeleton. *J Cell Biol* 140:1211–1225, 1998
31. Clark SF, Molero JC, James DE: Release of insulin receptor substrate proteins from an intracellular complex coincides with the development of insulin resistance. *J Biol Chem* 275:3819–3826, 2000
32. Whitehead JP, Clark SF, Urso B, James DE: Signalling through the insulin receptor. *Curr Op Cell Biol* 12:222–228, 2000
33. Alessi DR, Andjelkovic M, Caudwell B, Cron P, Morrice N, Cohen P, Hemmings BA: Mechanism of activation of protein kinase B by insulin. *EMBO J* 15:6541–6551, 1996
34. Coffer PJ, Jin J, Woodgett JR: Protein kinase B (c-Akt): a multifunctional mediator of phosphatidylinositol 3-kinase activation. *Biochem J* 335:1–13, 1998
35. Foran PGP, Fletcher LM, Oatey PB, Mohammed N, Dolly JO, Tavaré JM: Protein kinase B stimulates the translocation of GLUT4 but not GLUT1 or transferrin receptors in 3T3–L1 adipocytes by a pathway involving SNAP-23, synaptobrevin-2, and/or cellubrevin. *J Biol Chem* 274:28087–28095, 1999
36. Hill MM, Clark SF, Tucker DF, Birnbaum MJ, James DE, Macaulay SL: A role for protein kinase B/Akt2 in insulin-stimulated GLUT4 translocation in adipocytes. *Mol Cell Biol* 19:7771–7781, 1999
37. Wang O, Somwar R, Bilan PJ, Liu Z, Jin J, Wwoodgett JR, Klip A: Protein kinase B/Akt participates in GLUT4 translocation by insulin in L6 myoblasts. *Mol Cell Biol* 19:4008–4018, 1999
38. Rea S, James DE: Moving GLUT4: the biogenesis and trafficking of GLUT4 storage vesicles. *Diabetes* 46:1667–1677, 1997
39. Cheung PCF, Salt IP, Davies SP, Hardie DG, Carling D: Characterization of AMP-activated protein kinase γ-subunit isoforms and their role in AMP binding. *Biochem J* 346:659–669, 2000
40. Houmard JA, Hickey MS, Tyndall GL, Gavigan KE, Dohm GL: Seven days of exercise increase GLUT-4 protein content in human skeletal muscle. *J Appl Physiol* 79:1936–1938, 1995
41. Yip J, Facchini FS, Reaven GM: Resistance to insulin-mediated glucose disposal as a predicator of cardiovascular disease. *J Clin Endocrinol Metab* 83:2773–2776, 1998
42. Laasko M: Hyperglycemia and cardiovascular disease in type 2 diabetes. *Diabetes* 48:937–942, 1999
43. White MF, Kahn CR: The insulin signalling system. *J Biol Chem* 269:1–4, 1994
44. Inoue G, Cheatham B, Emkey R, Kahn CR: Dynamics of insulin signalling in 3T3–L1 adipocytes. *J Biol Chem* 273:11548–11555, 1998
45. Pessin JE, Thurmond DC, Elmendorf JS, Coker KJ, Okada S: Molecular basis of insulin stimulated GLUT4 vesicle trafficking: location! location! location! *J Biol Chem* 274: 2593–2596, 1999
46. Martin L, Shewan A, Millar CA, Gould GW, James DE: Vesicle associated membrane protein-2 (VAMP2) plays a specific role in the insulin-dependent trafficking of the facilitative glucose transporter GLUT4 in 3T3–L1 adipocytes. *J Biol Chem* 273:1444–1452, 1998
47. Martin S, Tellam J, Livingstone C, Slot JW, Gould GW, James DE: The glucose transporter (GLUT4) and vesicle-associated membrane protein (VAMP2) are segregated from recycling endosomes in insulin-sensitive cells. *J Cell Biol* 134:625–635, 1996
48. Volchuk A, Wang Q, Ewart HS, Liu Z, He L, Bennett MK, Klip A: Syntaxin 4 in 3T3–L1 adipocytes: regulation by insulin and participation in insulin-dependent glucose transport. *Mol Biol Cell* 7:1075–1082, 1996
49. Volchuk A, Mitsumoto Y, He L, Lui Z, Habermann E, Trimble WS, Klip A: Expression of vesicle-associated membrane protein 2 (VAMP2)/synaptobrevin II and cellubrevin in rat skeletal muscle and in a muscle cell line. *Biochem J* 304:139–145, 1994
50. Olson AL, Knight JB, Pessin JE: Syntaxin 4, VAMP2, and/or VAMP3/Cellubrevin are functional target membrane and vesicle SNAP receptors for insulin-stimulated GLUT4 translocation in adipocytes. *Mol Cell Biol* 17:2425–2435, 1997
51. Cheatham B, Volchuk A, Kahn CR, Wang L, Rhodes C, Klip A: Insulin-stimulated translocation of GLUT4 glucose transporters requires SNARE-complex proteins. *Proc Natl Acad Sci U S A* 93:15169–15173, 1996
52. Smart EJ, Graf GA, McNiven MA, Sessa WC, Engelman JA, Scherer PE, Okamoto T, Lisanti MP: Caveolins, liquid-ordered domains and signal transduction. *Mol Cell Biol* 19:7289–7304, 1999
53. Gustavsson J, Parpal S, Karlsson M, Ramsing C, Thorn H, Borg M, Lindroth M, Peterson KH, Magnusson K-E, Strålfors P: Localization of the insulin receptor in caveolae of adipocyte plasma membrane. *FASEB J* 13:1961–1971, 1999
54. Scherer PE, Lisanti MP, Baldini G, Sargiacomo M, Mastick CC, Lodish HF: Induction of caveolin during adipogenesis and association of GLUT4 with caveolin-rich vesicles. *J Cell Biol* 127:1233–1243, 1994
55. Saltiel AR: Diverse signaling pathways in the cellular actions of insulin. *Am J Physiol* 270:E375–E385, 1996.